

Spatiotemporal variations of snow cover in Mt. Norikura, the Northern Japanese Alps

*Motoshi Nishimura^{1,4}, Rui Tanaka^{2,5}, Akihiko Sasaki³, and Keisuke Suzuki²

¹ Interdisciplinary Graduate school of Science and Technology, Shinshu University

² Faculty of Science, Shinshu University

³ Department of Geography and Environmental Studies

Current affiliation:

⁴ National Institute of Polar Research

⁵ Kankyomirai Co., Ltd.

Address:

^{1,2} 3-1-1 Asahi, Matsumoto, Nagano, 390-8621, Japan

³ 4-28-1 Setagaya, Setagaya-ku, Tokyo, 154-8515, Japan

⁴ 10-3 Midori-cho, Tachikawa, Tokyo, 190-8518, Japan

⁵ 4010-5 Wada, Matsumoto, Nagano, 390-1242, Japan

*Corresponding Author: Motoshi Nishimura (nishimura.motoshi@nipr.ac.jp)

Abstract

Snow cover is a major factor influencing the local atmospheric environment. Snow depth in mountainous areas varies significantly owing to the effects of humid air advection and topography. However, snow cover distribution in the mountainous areas of Japan has not yet been quantitatively studied. In this study, in situ meteorological observation data from 2013/14 to 2019/20 on the eastern and western slopes of Mt. Norikura (Northern Japanese Alps) and the surrounding synoptic weather conditions were analyzed. The results showed that snow depth on the eastern slope was greater than that on the western slope. The maximum and minimum snow depths at all sites during the observation period were greater than 229 cm and almost 96 cm, respectively. The variation in annual maximum snow depth was less at the high-elevation site than at the low-elevation site. This is because lower air temperatures at higher elevations make the environment more conducive to stable snowfall and snow accumulation. In addition, variations in snow accumulation with elevation have unique characteristics: 1) the amount of snow accumulation showed a contrast, in that large accumulations in high elevation areas on the east slope and small accumulations in high elevation areas on the west slope are a result of strong westerly winter monsoon wind conditions; and 2) a cyclone along the Japanese south coast, possibly providing easterly air mass advection with a cyclonic circulation towards the slope of Mt. Norikura, supplies much snowfall in the low elevation areas on the east slope. The complex mountainous terrain and atmospheric advection path have created a unique spatiotemporal variation in the snow cover distribution on Mt. Norikura.

Keywords: seasonal snow cover, snowfall, alpine region, in-situ observation, Japanese Alps

1. Introduction

Snow is an important water source in the Northern Japanese Alps (Hida Mountains), which experience significant snowfall resulting from a strong winter monsoon pattern originating in continental Siberia. The northwesterly wind, which is rich in water vapor generated by the warm superficial Tsushima Current (Kurooka, 1957; Ninomiya, 1968), provides a warm and humid

air mass to the coastal area of the Sea of Japan. The humid air mass provided by the winter monsoon advects over the Northern Japanese Alps (Estoque and Ninomiya, 1976), resulting in significant snowfall in the windward area of the Alps.

Japanese alpine regions are located at low latitudes in relatively warmer regions. In such locations, even small temperature changes can alter snow conditions. Snow depth in Japan is predicted to decrease with global warming (Inoue and Yokoyama, 2003; Hara et al., 2008). However, previous studies

used data from low-elevation sites, and the snowfall amount was predicted to increase in higher-elevation mountainous regions (Suzuki, 2012; Kawase et al., 2020). Furthermore, regional climate model simulations have reported that global warming could lead to heavier snowfall in the mountainous regions of central Japan than in the coastal areas of the Sea of Japan (Sasai et al., 2019). Because of the temperate climate and high spatial undulations of Japan's topography, the high spatial variability of snowy environments has been reported as a consequence of global warming.

Significant spatial variability in snow cover in mountainous areas contributes to the complexity of alpine environmental systems (climate, topography, and ecosystems). For example, Mott et al. (2015) and Uehara et al. (2020) reported the relationship between a local wind system and snow cover distribution in alpine regions, which is caused by the spatiotemporal variation of snow cover forcing turbulent sensible heat flux from snow cover to the atmosphere. Because of the complex terrain and steep elevation gradients, snow cover has a significant impact on vegetation variability and the near-surface atmospheric environment in alpine environments. Moreover, the snow cover duration, which depends on elevation, also regulates the leafing period (Oguma et al., 2019). It is necessary to evaluate the spatial variability of snow cover to monitor and understand alpine environments that are composed of multiple natural elements.

The spatial variation in the precipitation was significant. In mountainous regions, winter precipitation accumulation depends on annual variations in precipitation rather than on annual air temperatures (Yamaguchi et al., 2011). This is because the large spatial variation of surface air temperatures due to complex terrain possibly makes the precipitation phase variable. Many studies surveying the spatial variability of snow cover in the Japanese alpine region have been conducted since the 1950s (e.g. Yoshida, 1960; Suizu et al., 1978; Matsuyama, 1998). In addition, long-term snow depth observational point data in the alpine region were reported by Suzuki and Sasaki (2019) and Nishimura et al. (2019), contributing to snow observation data in the Northern Japanese Alps region under recent intensifying climate change conditions. However, Nishimura et al. (2019) only analyzed a single point of data in detail, and Suzuki and Sasaki (2019) only compiled point data for a broad area in the Japanese Alps region. To understand the characteristics of snow cover distribution in rugged mountainous regions, it is necessary to conduct an analysis based on multiple in situ observation data that can consider topographic effects on a local scale. Nevertheless, in this context, the difficulty of installing and maintaining meteorological instruments, coupled with the lack of a network to aggregate fragmented reported data, has made it difficult to provide a sufficient volume and density of information to understand the dynamics of the Japanese alpine region for advancing environmental science.

The objective of this study was to reveal spatial and temporal variations in the seasonal snow cover accumulation–ablation process based on in situ observation data measured at multiple sites in the Northern Japanese Alps region. An investigation of interannual snow depth and snowfall variability at different elevations on the eastern and western slopes of Mt. Norikura was conducted over seven seasons. This observation network provides a variety of observational data, which enables us to discuss 1) the long-term fluctuation of annual snow depth and snow-covered duration, 2) the variation of the long-term snow depth fluctuation with elevation, and 3) the dependence of the snow accumulation variability with location (on the west-east slope). We confirm and discuss using the observation data that the snow amount is dependent on elevation, and whether its elevational variation differs based on slope direction. The Japanese Alps region, including Mt. Norikura, is at the southern margin of the temperate cryosphere in the Northern Hemisphere. Snow environmental variables in these mid-latitude alpine areas may show more pronounced trends of change with climate change than those in the high-latitude cryosphere and polar regions. This study contributes to our understanding of the snow/ice environment in the mid-latitude temperate cryosphere under global warming conditions by analyzing long-term snow cover data from Mt. Norikura.

2. Method

1) Site description

Mt. Norikura, which consists of several high mountain peaks, is located at the southern edge of the Northern Japanese Alps. One of these peaks continues for 5 km in a north-south direction, with Mt. Kengamine (3026 m a.s.l.) as its main peak. The subalpine zone vegetation of Mt. Norikura, which ranges from 1600–1700 m a.s.l. to 2400–2500 m a.s.l., is dominated by deciduous broad-leaved species (e.g., *Betula ermanii*) and evergreen needle-leaved vegetation (e.g., *Abies veitchii*, and *Abies mariesii*). Over 100 cm of seasonal snow cover forms at the bottom of this subalpine zone every year from mid-November to early March/late April (Suzuki and Sasaki, 2019; Nishimura et al., 2019). At elevations above 2500 m a.s.l., the surface of the slopes commonly shows a convex or rectilinear profile and remarkably even cross profile. These slopes named periglacial smooth slope, consist of gravel and sand, which are formed the periglacial processes (e.g., frost weathering). On these slopes, vegetation comprises a dwarf forest dominated by *Vaccinium vitis-idaea* and *Pinus pumila* communities.

2) Meteorological observation setting and data treatment

Meteorological observations were conducted at five sites (E-1590, E-1810, E-1990, E-2200, and E-2360) on the eastern slope and at three sites (W-1940, W-2200, and W-2500) on the western

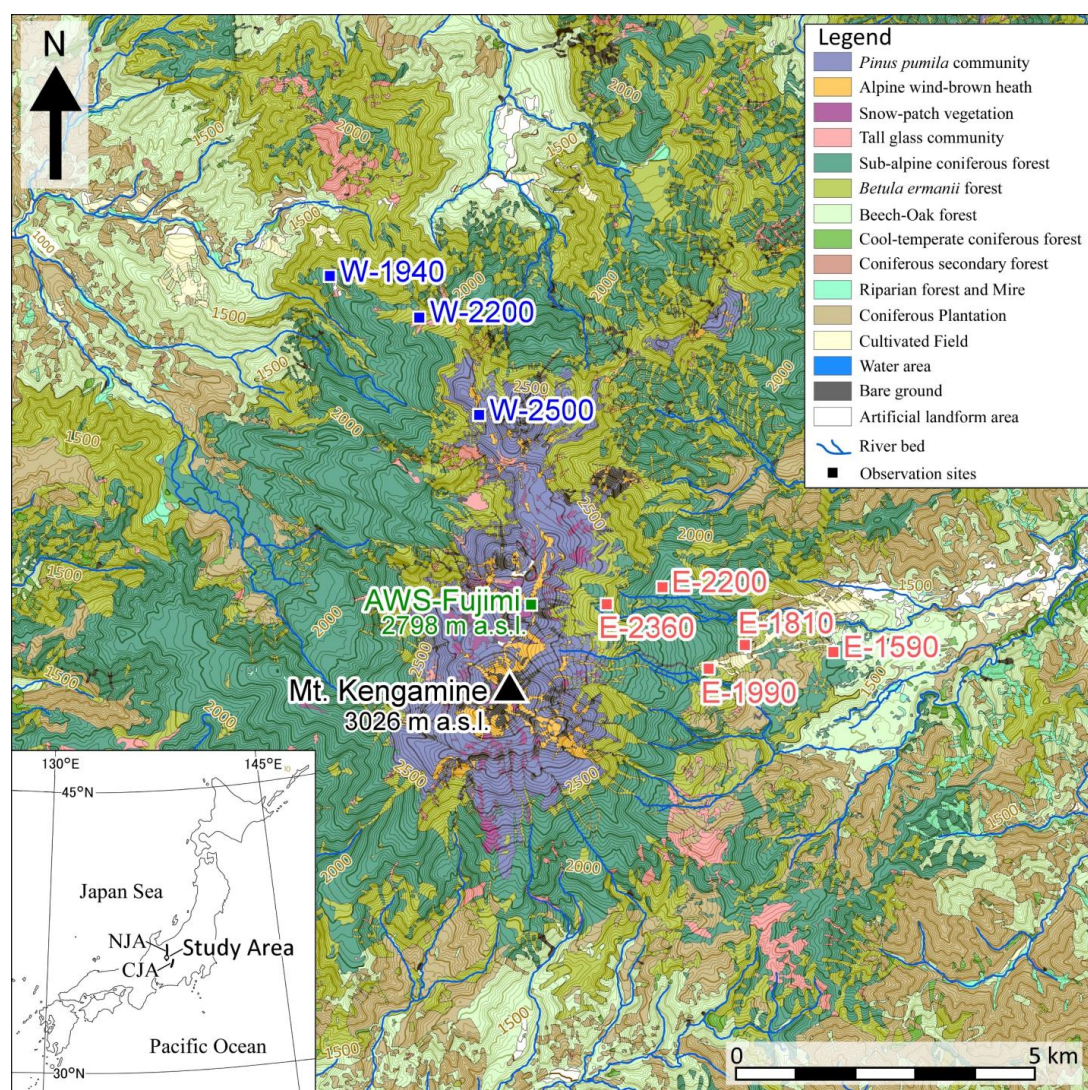


Fig. 1 Map of Mt. Norikura, showing the observation site locations, surrounding topography, and vegetation. Thick two lines with NJA (Northern Japanese Alps) and CJA (Central Japanese Alps) in the wide-area map represent those locations, which includes targeted study area. The terrain contour intervals for the thick and standard lines were set to 100 and 20 m, respectively. This map was modified from GIS data of a 1:25000 scale vegetation map created by the Biodiversity Center of Japan, Ministry of the Environment (<http://gis.biodic.go.jp/webgis/>).

slope of Mt. Norikura (Fig. 1). The observational data from Nishimura et al. (2019), Suzuki and Sasaki (2019), and Uehara et al. (2020) were used in this study. A data logger was used to record hourly air temperature [$^{\circ}\text{C}$] and snow depth [cm]. In addition to observations on the western and eastern slopes, an automatic weather station (AWS-Fujimi: 2798 m a.s.l.) was operated on the ridge of Mt. Fujimi-dake, a sub-peak of Mt. Norikura. The detailed specifications for the AWS of E-1590 and AWS-Fujimi are provided by Suzuki and Sasaki (2019) and Nishimura et al. (2018). Tables 1 and 2 list the observation sites and the instruments, respectively. Figure 2 provides two overviews of the observational instruments. The air temperature was measured using a thermometer (TR-5106, T&D) but at E-1590, W-1940,

Table 1. List of observation site and observation components.

Site	Elevation m a.s.l.	Observation element		
		Air temp. $^{\circ}\text{C}$	Snow depth cm	Wind speed m s^{-1}
E-1590	1590	○	○	○
E-1810	1810	○	○	
E-1990	1990	○	○	
E-2200	2200	○	○	
E-2360	2360	○	○	
W-1940	1940	○	○	
W-2200	2200	○	○	
W-2500	2500	○	○	
AWS-Fujimi	2798	○		○

Table 2. Sensor specifications for each observation instrument.

Observation element		Instrument		Accuracy
Air temperature	degree C	Delta OHM	HD9817T1R	$\pm 0.2^{\circ}\text{C}$
		T&D	RTR-502, TR-5106	$\pm 0.3\text{--}0.5^{\circ}\text{C}$
Snow depth	m	North one	KADEC21-SNOW	$\pm 1\text{cm}$
Wind speed	m s^{-1}	YOUNG	Model 05103 Wind Monitor	$\pm 0.3 \text{ m s}^{-1}$

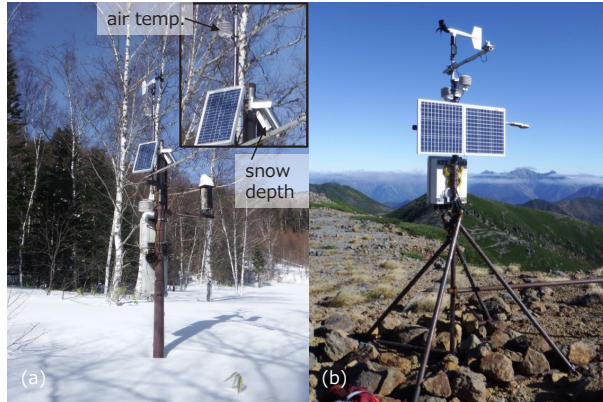


Fig. 2 Meteorological observation instruments at the (a) E-1590 and (b) AWS-Fujimi sites. Other sites recorded air temperatures in a natural ventilation shelter, and snow depth on a flat surface, such as E-1590.

and AWS-Fujimi a thermometer with a HD9817T1R sensor (Delta OHM) was used. Each thermometer was housed in a naturally ventilated shelter. Snow depth was measured using a laser range meter (KADEC21-SNOW, North One).

Hourly data from each winter season from November 1, 2013, to June 21, 2020, were analyzed. The quality of each data point was ensured owing to the quality control of the data operator. The quality control manually masks erroneous data records that are increased or decreased by several tens of centimeters from one hour before, or data that changes in a spike-like manner. These data could be attributed to the attachment of snow, icing, riming, and data logger malfunction. For these reasons, the data were missing in some cases. A data completeness requirement of 80% was applied when calculating the daily mean temperature and the accumulated snow depth for each winter season. Daily values that did not satisfy the data completeness requirements were considered to be missing. The daily snow depth was defined as the maximum snow depth per day. In this study, the day boundary was set to 00:00 (JST). This study defined the daily snowfall amount [cm] as the difference in daily snow depth as follows:

$$\text{snowfall amount} = (sd_i - sd_{i-1}), \quad (1)$$

where sd is the daily snow depth data and i represents a daily time step. Note that snow surface degradation due to compression was ignored in this study, because the amount cannot be estimated

using observational data.

The synoptic weather conditions around Japan were classified into six patterns based on the classification of Yoshino and Kai (1975): I, typical winter monsoon; II-a, south-coast cyclone; II-b, Japan Sea cyclone; II-c, double cyclone; II-d, atmospheric pressure trough; and III, anticyclone. Hereafter, weather classifications are written as pattern numbers. The classification was conducted using a synoptic weather chart at 09:00 JST published by the Japan Meteorological Agency. When more than one synoptic weather pattern appeared, the weather pattern that had the largest impact on Mt. Norikura was selected.

3. Results

1) Snow depth observation data

The seasonal snow depth fluctuations between 2013/14 and 2019/20 on the eastern and western slopes of Mt. Norikura are shown in Fig. 3. Although some of the observation data at E-1590 have already been reported by Suzuki and Sasaki (2019) and Nishimura et al. (2019), some brief reports are also provided here, and are summarized in Table 3. The fluctuations demonstrate that maximum and minimum accumulations were observed during the winters of 2014/15 and 2015/16, respectively. On the east slope sites, the maximum snow depths were 237 (E-1590), 290 (E-1810), 277 (E-1990), 287 (E-2200), and 370 cm (E-2360), whereas the minimum snow depths were 96 (E-1590), 117 (E-1810), 145 (E-1990), 178 (E-2200), and 265 cm (E-2360), respectively. On the western slope, the maximum snow depths were 229 (W-1940) and 280 cm (W-2200), with minimum depths of 108 (W-1940) and 155 cm (W-2200), respectively.

The snow depth on the eastern slope was greater than that on the western slope (Figs. 3 and 4). When sites at the same altitude were compared, the annual maximum snow depth at the E-2200 site fluctuated from 178 cm to 287 cm, except during the 2015/16 winter season. In contrast, at the W-2200 site, it fluctuated from 155 to 280 cm, except for 2014/15. A similar trend was observed between the E-1990 and W-1940 sites, with almost equivalent elevations. The mean seasonal maximum snow depths throughout the observation period on each slope (Fig. 4) also clearly show the snow depth difference between the slopes, which was larger on the east than the west slope sites.

Seasonal snow cover disappeared between early April and late May at the E-1590 site, and between early June and early July at the E-2360 site. Conversely, at the W-1940 site, it was between mid-April and early May and between early May and early June at the W-2200 site. The late disappearance (in early July) of seasonal snow cover at the E-2360 site occurred during the 2013/14, 2014/15, and 2016/17 winter seasons. In addition, the late disappearance (mid-May) of seasonal snow cover at the W-1940 site was recorded during 2013/14, 2016/17, 2018/19, and 2019/20. Similarly, it occurred in early June in 2013/14,

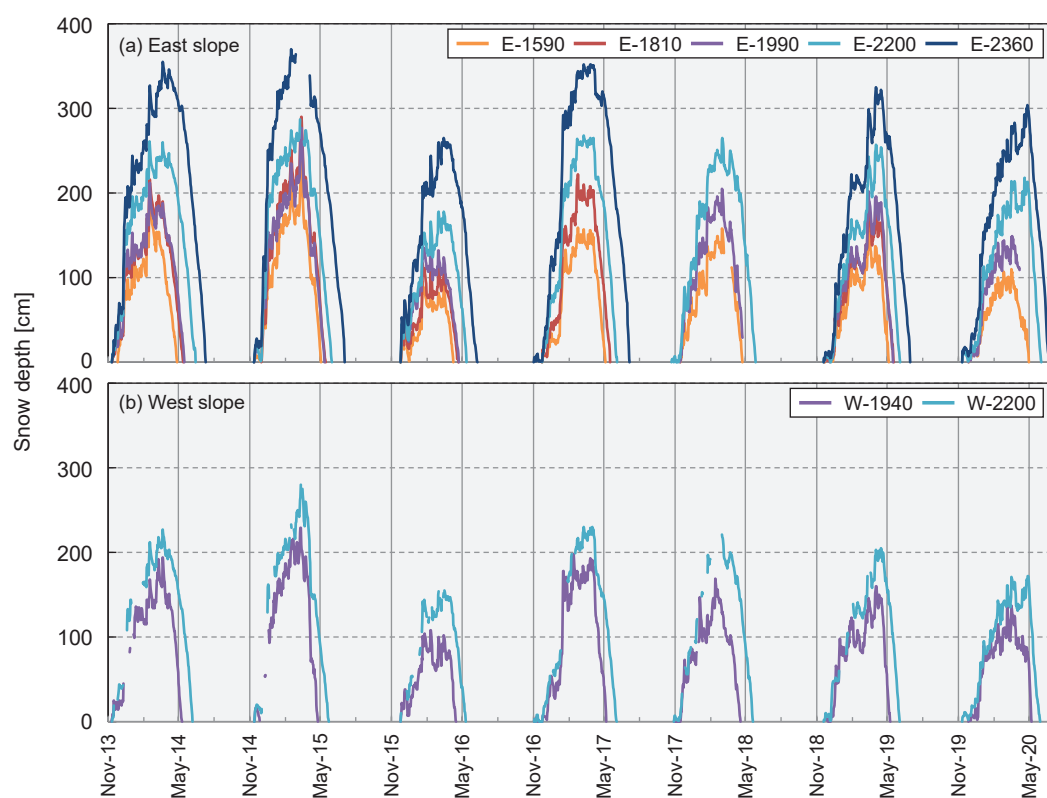


Fig. 3 Snow depth fluctuation during the 2013/14 to 2019/20 winter seasons on the (a) east and (b) west slopes of Mt. Norikura.

Table 3. List of annual maximum snow depth at every site and year.

Year	Annual maximum snow depth [cm]							
	West slope			East slope				
	W-1940	W-2200	W-2500	E-2360	E-2200	E-1990	E-1810	E-1590
2013/14	194	227	N.D.	355	261	212	216	204
2014/15	229	280	263	370	287	277	290	237
2015/16	108	155	168	265	178	145	117	96
2016/17	198	230	246	352	268	N.D.	222	159
2017/18	169	221	254	N.D.	265	205	N.D.	158
2018/19	160	205	236	325	257	202	192	160
2019/20	137	172	N.D.	304	218	149	N.D.	110
ave.	170.7	212.9	233.4	328.5	247.7	198.3	207.4	160.6
SD	37.6	38.1	33.9	35.6	34.3	44.2	55.7	45.5

N.D.: No Data (missing record)

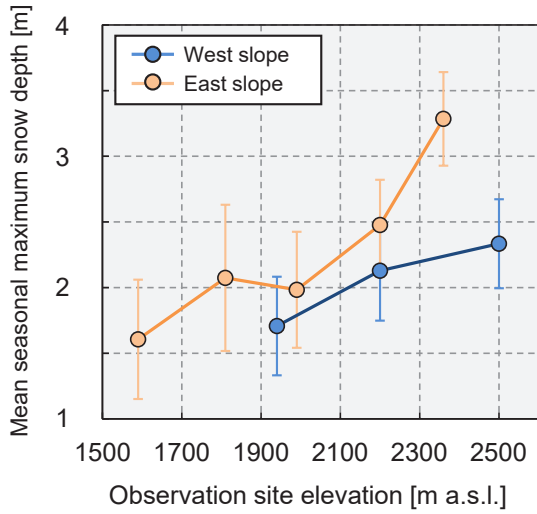


Fig. 4 Mean seasonal maximum snow depth during the observation period (2013/14–2019/20) at each site. The orange and blue plots indicate the observation data on the east and west slope sites, and the error bars represent ± 1 standard deviation of each data point.

2016/17, and 2018/19 at the W-2200 site. The time of snow cover disappearance at each site varied annually.

2) Relationship between the seasonal maximum snow depth and elevation

Temporal variations in the daily mean air temperature, maximum snow depth, and snowfall amount at sites E-1590, E-2200, W-1940, and W-2200 in 2018/19 are shown in Fig. 5. The seasonal maximum snow depth at E-1590 site was observed on March 14, 2019 (Figs. 4 and 5). The daily mean air temperature at

this site was also above freezing from mid-March, and the snow depth decreased during the same period (Fig. 5a). At the E-2200 site, the seasonal maximum snow depth was observed on April 2, 2019 (Fig. 6), and daily mean air temperatures above freezing were frequently observed from mid-April (Fig. 5b). After March 14, snowfall at the E-1590 and E-2200 sites was observed for eight and 12 days, respectively, in the 2018/19 winter season.

On the western side, the seasonal maximum snow depth at the W-1940 site was recorded on April 4, 2019 (Fig. 6). Daily mean air temperatures above freezing at this site were frequently observed after mid-April, and the snow depth decreased gradually thereafter (Fig. 5c). Conversely, for the W-2200 site, daily mean air temperatures above freezing only occurred after late April (Fig. 5d).

The snow-covered period and day of observation of the seasonal maximum snow depth are summarized in Fig. 6. This indicates that the maximum snow depth tended to be recorded at almost the same time at the E-1590, E-1810, and E-1990 sites. In 2013/14, 2015/16, and 2016/17, the seasonal maximum snow depth was recorded between mid-January and February at sites E-1590 and E-1810. In contrast, the maximum snow depth was observed from mid-February to mid-March at the E-2200 site, and between early and late March at the E-2360 site. The maximum snow depths were observed later in 2018/19 and 2019/20 than in other years. The maximum snow depths at the E-1590, E-1810, and E-1990 sites were observed in mid-March, and at the E-2200 and E-2360 sites in April.

The maximum snow depth at the W-1940 site was recorded between mid-January and mid-February. In addition, the maximum snow depth was observed at the W-2200 site from early March to early April. In contrast, the seasonal maximum was recorded in early April and mid-March at the W-1940 site, during

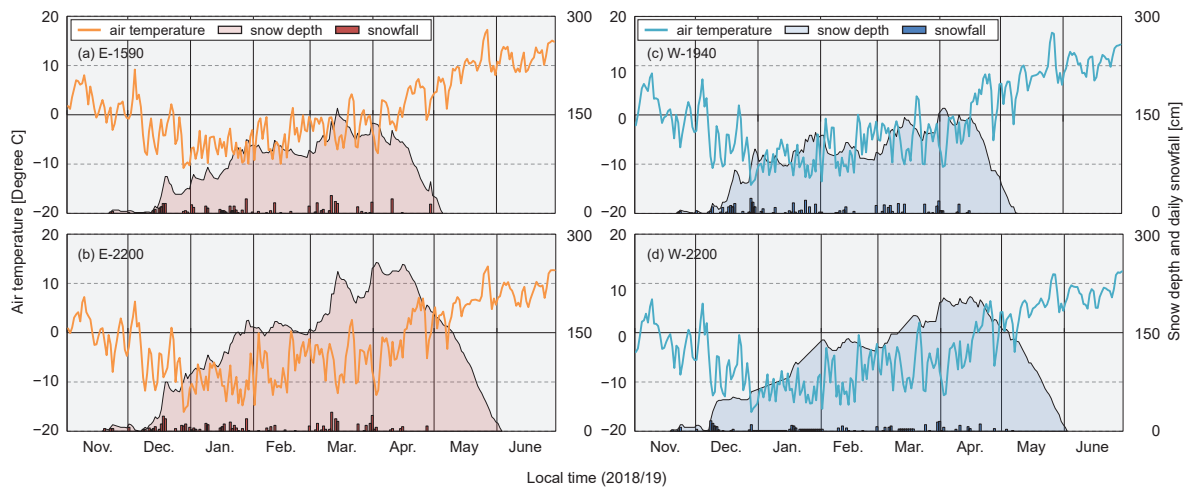


Fig. 5 Inter-seasonal variations in daily mean air temperature, daily maximum snow depth, and daily accumulative snowfall amount at sites (a) E-1590, (b) E-2200, (c) W-1940, and (d) W-2200 during the 2018/19 winter.

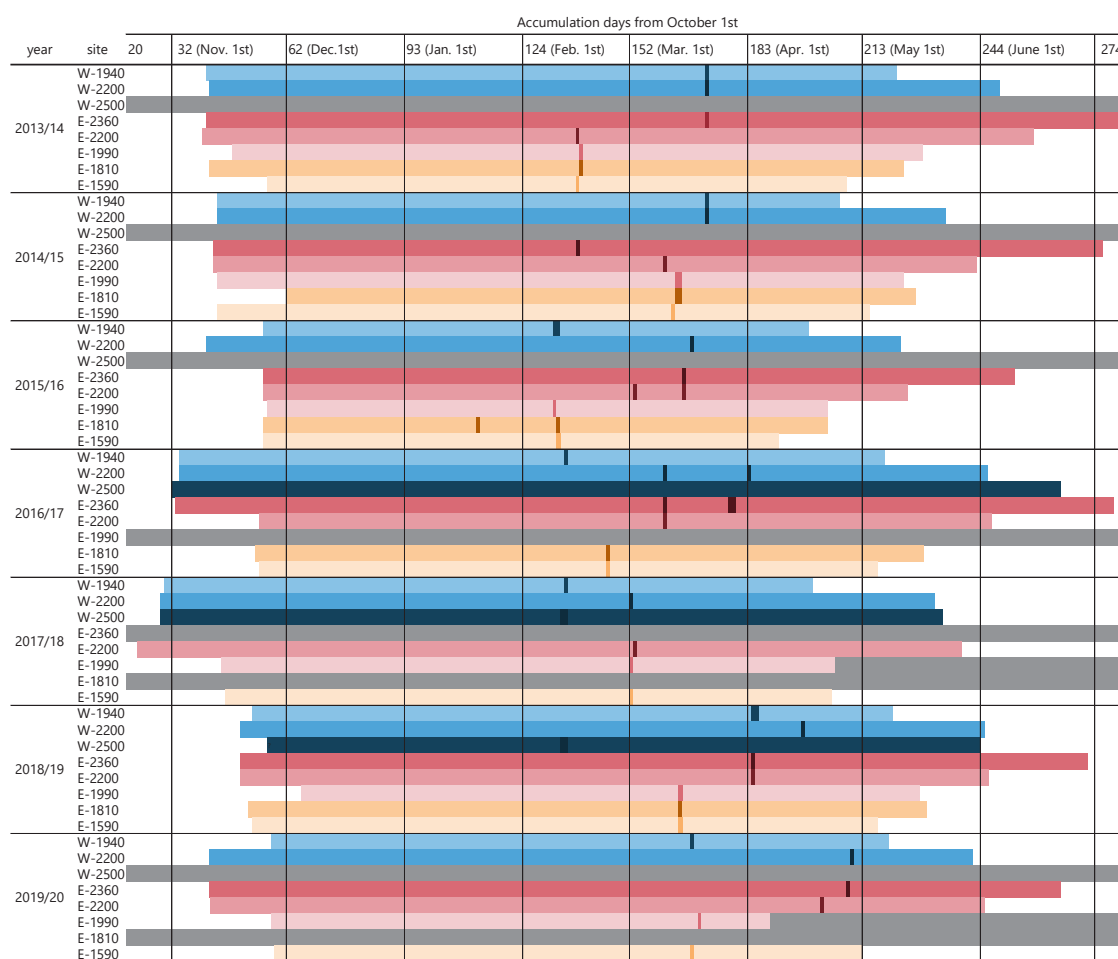


Fig. 6 The observation period with snow cover and the day of maximum snow depth at each site between 2013/14 and 2019/20. Each colored crossbar represents the snow-covered period, and a deep-colored day indicates that the day maximum snow depth was recorded. The gray shaded period represents missing data. The horizontal axis is a daily timescale representing the accumulation days from October 1st. However, note that the date shown next to the accumulation days is delayed by one day in the leap years (2016 and 2020).

2015/16 and 2016/17, respectively. At W-2200, the maximum snow depth was recorded in mid-April, which was later than that in the other winter seasons.

3) Spatial snowfall amount variation due to synoptic weather state

The average frequency of each weather pattern from 2013/14 to 2019/20 is shown in Fig. 7. Weather Pattern I was dominant in December and January for over half a day each month. From February, the frequency of Pattern I decreased, and the frequency of Patterns II-a and III increased. No remarkable trends were observed in the other patterns.

Figure 8 shows the averaged ratios of snowfall occurring during synoptic weather conditions classified into six patterns

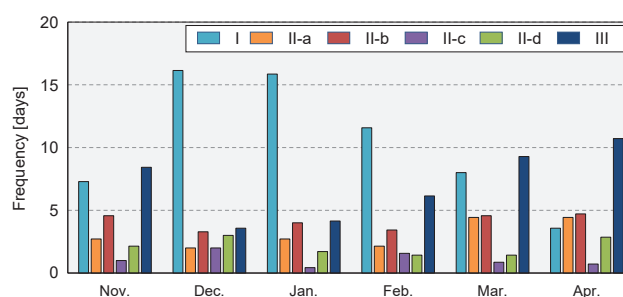


Fig. 7 The average frequency of synoptic weather states around Japan from the 2013/14 to 2019/20 winter seasons (November to April each year). Numbers I to III indicate synoptic weather patterns; I, typical winter monsoon pattern; II-a, south-coast cyclone; II-b, Japan sea cyclone; II-c, double cyclone; II-d, atmospheric pressure trough; III, anticyclone.

(see Chapter 2) in relation to the accumulated snowfall amount in December and February during the observation periods. The average and cumulative snowfall amounts for daily snowfall events during the seven winter seasons are illustrated in Fig. 9a and b. Figure 8a shows that significant snowfall in December was supplied by weather pattern I at every site. On the west slope, snow accumulation due to weather pattern I was small at the high-elevation sites in December (Fig. 9a and c). In contrast, it was large at the high-elevation site on the eastern slope during the same period. In contrast, it was large at the high-elevation site on the eastern slope during the same period (Fig. 9a and c). Compared to the results in December, in February the snowfall amount of both single snowfall events and accumulated for all seasons supplied in the pattern I condition decreased, and those due to pattern II-a increased (Figs. 7 and 8). Subsequently, snow accumulation due to weather pattern II-a in February was greater on the eastern than the western slope (Fig. 9d).

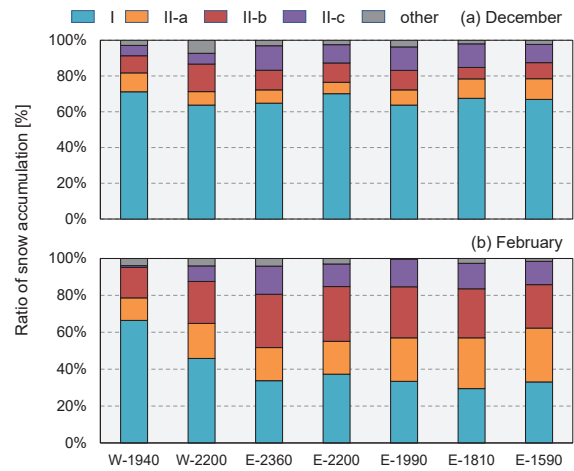


Fig. 8 Average ratio of the snow accumulation amount for each synoptic weather pattern to the total snow accumulation amount for seven winters (from November to April in 2013/14–2019/20) in (a) December and (b) February.

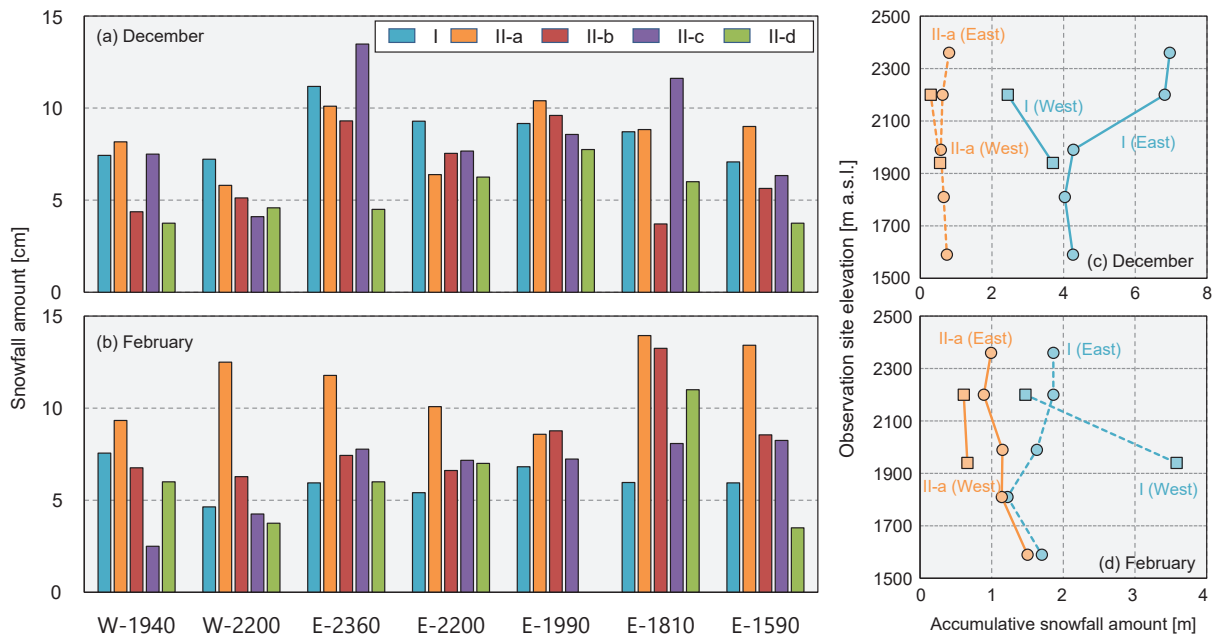


Fig. 9 (a and b) Average snowfall amount due to a single snowfall event for seven winter seasons (November to April in 2013/14–2019/20). The snowfall amount was calculated by dividing the accumulated snowfall amount for each winter by the frequency of snowfall events with increasing snow depth for each synoptic weather pattern. The relationship between the elevation of the observation sites and the accumulative snowfall amount through the observation period on each slope and site classified with synoptic weather patterns I and II-a. Circle and square plots represent snowfall amounts at the sites on the east and west slopes, respectively.

4. Discussion

1) Air temperature controls the seasonal maximum snow depth and snow-covered period

Air temperature is an important factor that influences snow

accumulation. The observational data shown in Fig. 3 indicate that the seasonal snow depth on the east slope at Mt. Norikura was greater at higher elevation sites. Nishimura et al. (2019) reported long-term meteorological and seasonal snow cover observations from the winter seasons between 2002/03 and 2016/17 at the E-1590 site. The high air temperatures seen in this previous

study continued from November to January in the 2015/16 winter season, which prevented snow accumulation. This study also indicated that high air temperature conditions continued during the 2015/16 winter season, leading to less snow cover formation during this period. This reduced snow cover formation was also observed at other observation sites on Mt. Norikura (Fig. 3). The lowest seasonal snow depth was recorded during 2015/16 at every observation site.

Fluctuations in the seasonal maximum snow depth during the observation period were relatively small at high-elevation sites on both slopes. At the E-2360 and W-2500 sites, the maximum snow depths during the observation period were 370 cm and 263 cm, and the minimum seasonal maximum snow depths were 265 cm and 168 cm, respectively (Fig. 3 and Table 3). In contrast, low-elevation sites, such as the E-1590 site, had large variations in the maximum snow depth and snow-covered periods (Nishimura et al., 2019). The study and Table 3 show the maximum difference in seasonal maximum snow depth between the 2002/03 and 2016/17 winter seasons, and report a difference of 141 cm (maximum: 237 cm in 2014/15 and minimum: 96 cm in 2015/16). In addition, Kawase et al. (2020) simulated using a regional climate model, and indicated that snow cover decreases and snowfall intensity are weakened if the air temperature increases by 2 K or 4 K at low elevation areas (below 500 m a.s.l.). At high elevations (above 2000 m a.s.l. in the Northern Japanese Alps), a simulated 4 K rise in air temperature has the possibility of decreasing snow depth due to changes in precipitation phases.

The relationship between the air temperature and snow depth fluctuation is shown in Fig. 5. The difference in air temperature modified the precipitation phase and served as an indicator of the beginning of the ablation period at each site. The first day of the accumulation period occurred earlier, and the ablation period was initiated later, at high-elevation sites (Figs. 4 and 5). This was due to the decrease in the air temperature with increasing elevation. As shown in Fig. 5 (c and d), intermittent snowfall was observed until April in the 2018/19 winter season, and drastic snowmelt started late at the W-2200 site because a significant increase in air temperature did not occur. The maximum seasonal snow depth was observed in late April at the study site.

When the air temperature increases and precipitation changes from snow to rain, snowmelt accelerates (Marks et al., 1998; Nishimura et al., 2018). Although the threshold requirements for changing the precipitation phase remain unclear, the change in the precipitation phase appears to depend on air temperature, relative humidity, and atmospheric pressure (Dai, 2008; Ding et al., 2014; Jennings et al., 2018). The data required for the discussion of this topic are limited, because fewer precipitation phase measurements have been conducted, especially in alpine regions.

It can be suggested that the difference in air temperature due to elevation changes strongly influences seasonal snow cover duration and accumulation. In a low-temperature environment, the

precipitation phase does not tend to change to rain, meaning that more snow accumulation easily occurs in high-elevation areas. A longer snow-covered period was recorded, and there was less variation in the maximum snow depth throughout the observation period, at higher elevation sites (Figs. 3 and 5). Therefore, in low elevation areas with high temperatures, the snow cover duration and seasonal maximum snow depth are highly variable from year to year owing to the precipitation phase change, whereas in high elevation areas, the effect of precipitation change is relatively small, suggesting that snow cover and maximum snow depth may be more stable than in low elevation areas.

2) Spatial distribution of snowfall amount between the west and east slopes in Mt. Norikura

As shown in Fig. 3, the seasonal maximum snow depth is greater on the eastern than the western slope. As shown in Fig. 8, a large amount of snow was supplied by weather pattern I. This trend was more significant during December, while it was also apparent at the west-slope sites in February. The typical winter monsoon in Japan (weather pattern I) supplies a northwesterly wind that originates from the Eurasian continent and contains a warm and humid air mass (Kurooka, 1957; Magono et al., 1966; Ninomiya 1968). This circulation results in significant snow accumulation in the Northern Japanese Alps. A prevailing wind from one direction, such as the Japanese winter monsoon, and a mountain ridge orthogonal to the wind direction, such as the Japanese Alps, create a climate contrast (Viale et al., 2019). Humid climatic conditions prevail on the windward side of the Japanese Alps, whereas relatively dry conditions prevail on the leeward side (Nishimura et al., 2021). The same may be stated for snowfall. Although snow accumulation was generally greater in the windward areas, the observational data in this study and that of Tanaka and Suzuki (2008) indicate that the seasonal snow depth is greater on the eastern than the western slope during the monsoon weather pattern. Yamada et al. (1978) reported that the snow depth in the subalpine zone increases with elevation, and this trend is obscure above the tree line. The snow depth at higher elevations is lower than that in the subalpine zone, because snow cover is supposed to be eroded by strong wind in the above tree line area. These results indicate that the spatial distribution of snow depth in alpine region is strongly influenced by the wind and terrain. Therefore, despite the significant snow accumulation supplied by the winter monsoon (westerly wind) (Fig. 8), a greater snow depth was observed on the east slope, because it may be inferred that strong winter monsoon winds induced snow erosion on the west slope and redistributed it to the east slope of Mt. Norikura.

Moreover, snow accumulation resulting from weather pattern I on the west slope was small at higher elevation sites (Fig. 9a and c). The observed daily mean wind speed [m s^{-1}] and wind direction [degree] (using YOUNG 05103) at AWS-Fujimi in Fig.

10 illustrate a very strong westerly windy environment in winter, with a daily mean of over 15 m s^{-1} . As shown in Fig. 10a, a very strong wind continuously blows across the ridge of the Northern Japanese Alps due to the winter monsoon. Consequently, the snow distribution on both slopes of Mt. Norikura is significantly influenced by the Japanese winter monsoon, which induces snow erosion in the high-elevation area on the west slope and redistributes it to the high-elevation area on the east slope.

Mt. Norikura is strongly affected by the winter monsoon, because there are no prominent snow-producing mountains adjacent to the western slope. The south-coast cyclone had the greatest influence on snow accumulation at low elevations on the eastern slope of Mt. Norikura, compared with the high elevation sites on the east and west slope sites in February (Figs. 7 and 8). When we defined the low- and high-elevation sites on the eastern slope as E-1590, E-1810, and E-1990 (broad-leaved forest zone), and E-2200 and E-2360 (subalpine coniferous forest zone), respectively, the largest snowfall according to pattern II-a was supplied in the low-elevation sites, compared to the high-elevation sites and the western slope sites. The cyclone traveled along the southern coast of Japan. Its northeasterly cyclonic advection

provides a humid air mass attributed to the Pacific Ocean to the windward area (eastern slope region of Mt. Norikura), causing significant snow accumulation. We argue that such a unique snow accumulation characteristic of Mt. Norikura can be attributed to the location where major snow accumulation is supplied by the winter monsoon. In relatively inland areas in central Japan, the south-coast cyclone also supplies a large amount of snow accumulation on eastern slopes.

Additionally, the influence of strong westerly winds (winter monsoon) on the redistribution of snow cover may be relatively small at low-elevation sites on the east slope. A similar result was reported in a study in the Japanese Central Alps (Tanaka and Suzuki, 2008), and the AWS-Fujimi observation records in Fig. 10b also explained a lower frequency and weakness in the easterly windy condition at the ridge of Mt. Norikura. These data records suggest that there was less snow erosion, and redistribution did not occur from the east to west slope due to the south-coast cyclone. Therefore, it can be concluded that the low-elevation sites on the east slope were significantly affected by snow accumulation caused by the south-coast cyclone.

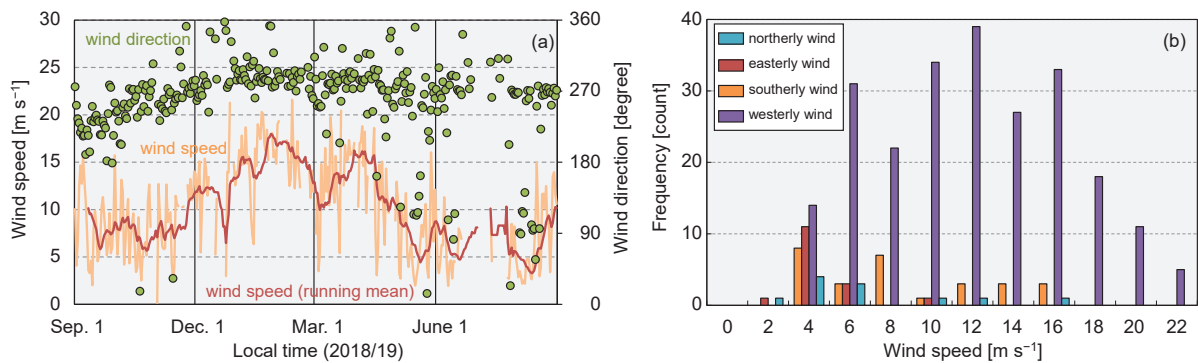


Fig. 10 (a) Fluctuation in daily mean wind speed (orange line), its 11-day running mean (red line), and daily mean wind direction (green plot). (b) Frequencies of daily mean wind speed for each daily mean wind direction range (wind direction [degree]; easterly: 45–135, southerly: 135–225, westerly: 225–315, northerly: 315–45). The bin of the wind-speed interval was 2 m s^{-1} . The data were attributed to observations at AWS-Fujimi from September 2018 to August 2019.

5. Conclusion

This study conducted seven winter season snow depth observations at multiple elevation sites on the eastern and western slopes of Mt. Norikura, the Northern Japanese Alps. Based on these observations, the following results were obtained.

(i) The snow depth and snow accumulation on the east and west slopes of Mt. Norikura's south-north ridge were dependent on slope aspect and elevation. Snow depth differences were larger on the east slope than the west slope (Fig.3). The annual maximum and minimum snow depths at all sites during the observation period were greater than 229 cm and 96 cm,

respectively. Although the snow-covered durations varied year-by-year, snow cover generally disappeared between mid-April and May at sites in the 1500–1600 m a.s.l. elevation zone, between mid-May and early June at mid-elevation sites (around 1800–1900 m a.s.l. zone), and between late May and late June at high elevation sites (above 2000 m a.s.l.) (Figs. 3 and 5).

(ii) In addition, the variation in seasonal maximum snow depth fluctuated with elevation. The difference between the maximum and minimum snow depths during the observation period was greater at high elevation sites (E-2360 and W-2500) than at low elevation sites (E-1590; 141 cm). This difference suggests that the lower air temperatures at higher elevations are

less likely to cause changes in the precipitation phase, and also decelerate melting of the snow layer, making the environment more conducive to stable snowfall and snow accumulation.

- (iii) According to the classification of synoptic weather conditions, a typical winter monsoon contributes significantly to snow accumulation. The strong winter monsoon may erode and redistribute the snow cover from the western slope to the eastern slope at least in December (Figs. 8a and 9). Moreover, the south-coast cyclone may provide easterly air mass advection with a cyclonic circulation to the eastern slope of Mt. Norikura. The average snowfall amount due to a single precipitation event was larger in the south-coast cyclone pattern than the winter monsoon pattern in February (Fig. 9b). Some investigations also suggested an apparent contrast in precipitation and snow cover between the windward and leeward regions (Tanaka and Suzuki, 2008; Viale et al., 2019).

This study suggests that synoptic weather patterns (a pass of air mass advection), differences in wind- and leeward slopes on the north-south ridge, and elevation strongly affect precipitation on Mt. Norikura. The large air temperature gradient in the alpine region significantly affects the precipitation phase. Therefore, the spatiotemporal snow cover variation in the Northern Japanese Alps would have been caused by typical Japanese weather patterns, due to the complex mountainous topography and atmospheric advection paths.

We believe that continuous in situ observations are important. Many analytical tools such as climate models and reanalysis have recently been developed. These products are useful for understanding natural mechanisms and large-scale spatial analysis. However, it should be noted that these products are applied based on observational data. Nevertheless, some in situ observational data contain missing data or characterize poorly understood phenomena. We expect that combining continuous steady observations with a high-resolution parameterization model will offer a reliable understanding of the natural organization of alpine regions.

6. Acknowledgement

This study is based on long-term observations from many field works. We acknowledge the tremendous contributions of all the people who have operated the AWSs' observation instruments and continuously managed the observation data. The significantly valuable indications and suggestions from the two anonymous reviewers were greatly appreciated, as they helped to improve the quality and value of this paper.

7. References

- Dai, A. (2008): Temperature and pressure dependence of the rain-snow phase transition over land and ocean. *Geophysical Research Letters*, **35**, 1–7, doi: 10.1029/2008GL033295.
- Ding, B., Yang, K., Qin, J., Wang, L., Chen, Y. and He, X. (2014): The dependence of precipitation types on surface elevation and meteorological conditions and its parameterization. *Journal of Hydrology*, **513**, 154–163, doi: 10.1016/j.jhydrol.2014.03.038.
- Estoque, M. A. and Ninomiya, K. (1976). Numerical simulation of Japan Sea effect snowfall. *Tellus*, **28**, 243–253, doi: 10.3402/tellusa.v28i3.10285.
- Hara, M., Yoshikane, T., Kawase, H. and Kimura, F. (2008): Estimation of the impact of global warming on snow depth in Japan by the Pseudo-Global-Warming method. *Hydrological Research Letters*, **2**, 61–64, doi: 10.3178/hrl.2.61.
- Inoue, S. and Yokoyama, K. (2003): Estimates of snowfall depth, maximum snow depth, and snow pack environments under global warming in Japan from five sets of predicted data. *Journal of Agricultural Meteorology*, **59**, 227–236, doi: 10.2480/agrm.59.227.
- Jennings, K. S., Winchell, T. S., Livneh, B. and Molotch, N. P. (2018): Spatial variation of the rain-snow temperature threshold across the Northern Hemisphere. *Nature Communications*, **9**, 1–9, doi: 10.1038/s41467-018-03629-7.
- Kawase, H., Yamazaki, T., Sugimoto, S., Sasai, T., Ito, R., Hamada, T., Kuribayashi, M., Fujita, M., Murata, A., Nosaka, M. and Sasaki, H. (2020): Changes in extremely heavy and light snow-cover winters due to global warming over high mountainous areas in central Japan. *Progress in Earth and Planetary Science*, **7**, doi: 10.1186/s40645-020-0322-x.
- Kurooka, H. (1957): Modification of Siberian the air mass caused by flowing out over the open sea surface of northern Japan. *Journal of the Meteorological Society of Japan*, **35**, 52–59.
- Magono, C., Kikuchi, K., Kimura, T., Tazawa, S. and Kasai, T. (1966): A study on the snowfall in the winter monsoon season in Hokkaido with special reference to low land snowfall (Investigation of natural snow crystals VI). *Journal of the Faculty of Science, Hokkaido University, Series 7, Geophysics*, **2**, 287–308.
- Marks, D., Kimball, J., Tingey, D. and Link, T. (1998): The sensitivity of snowmelt processes to climate conditions and forest cover during rain-on-snow: a case study of the 1996 Pacific Northwest flood. *Hydrological Processes*, **12**, 1569–1587, doi: 10.1002/(SICI)1099-1085(199808/09)12:10/11<1569::AID-HYP682>3.0.CO;2-L.

- Matsuyama, H. (1998): A review n the snow surveys conducted in mountainous regions in Japan to Distribution factors. *Journal of Japanese Society of Hydrology and Water Resources*, **11**, 164–174. (in Japanese with English abstract)
- Mott, R., Daniels, M. and Lehning, M. (2015): Atmospheric flow development and associated Changes in turbulent sensible heat flux over a patchy mountain snow cover. *Journal of Hydrometeorology*, **16**, 1315–1340, doi: 10.1175/jhm-d-14-0036.1.
- Ninomiya, K. (1968): Heat and water budget over the Japan Sea and the Japan islands in winter season. *Journal of the Meteorological Society of Japan*, **46**, 343–372, doi: 10.2151/jmsj1965.46.5_343.
- Nishimura, M., Sasaki, A. and Suzuki, K. (2018): Energy balance variation on the snow surface during the snow covered season in the Norikura highland, Japanese Alpine Area. *Bulletin of Glaciological Research*, **36**, 23–35, doi: 10.5331/bgr.18A02.
- Nishimura, M., Sasaki, A. and Suzuki, K. (2019): Long-term fluctuations, modelling and predictions of the snow accumulation and ablation process in Norikura highland: Study using an energy balance analysis and ablation models. *Journal of Geography (Chigaku Zasshi)*, **128**, 61–75, doi: 10.5026/jgeography.128.61. (in Japanese with English abstract)
- Nishimura, M., Sasaki, A. and Suzuki, K. (2021): Surface energy balance of snow cover in the Japanese Alps is similar to that in continental Alpine climates. *Environmental Research Communications*, **3**, 1–16, doi: 10.1088/2515-7620/abfcae.
- Oguma, H., Ide, R., Amagai, Y. and Hamada, T. (2019): Using a time-lapse camera network to monitor alpine vegetation phenology and snowmelt times. *Journal of Geography (Chigaku Zasshi)*, **128**, 93–104, doi:10.5026/jgeography.128.93. (in Japanese with English abstract)
- Sasai, T., Kawase, H., Kanno, Y., Yamaguchi, J., Sugimoto, S., Yamazaki, T., Sasaki, H., Fujita, M. and Iwasaki, T. (2019): Future projection of extreme heavy snowfall events with a 5-km large ensemble regional climate simulation. *Journal of Geophysical Research: Atmospheres*, **124**, 13975–13990, doi: 10.1029/2019JD030781.
- Suizu, S., Yamada, T. and Wakahama, G. (1978): Observations on depositional and melting processes of snow at different altitudes of Mt. Teine, Hokkaido. *Low Temperature Science Series A*, **37**, 47–54. (in Japanese with English summary)
- Suzuki, K. (2012): Snow hydrological study in the mountainous area and associated problems of meteorological observation. *Journal of Japanese Association of Hydrological Sciences*, **42**, 109–118, doi: 10.4145/jahs.42.109. (in Japanese with English abstract)
- Suzuki, K. and Sasaki, A. (2019): Meteorological observations in the Japanese Alps region. *Journal of Geography (Chigaku Zasshi)*, **128**, 9–19, doi: 10.5026/jgeography.128.9. (in Japanese with English abstract)
- Tanaka, M. and Suzuki, K. (2008): Spatial variability of snow water equivalent in a mountainous area of the Japanese Central Alps. *Journal of Geophysical Research: Earth Surface*, **113**, 1–11, doi: 10.1029/2006JF000711.
- Uehara, G., Nishimura, M., Sasaki, A. and Suzuki, K. (2020): The influence of snow cover for the local wind system on the east slope of Mt. Norikura. *Tenki*, **67**, 17–28, doi: 10.24761/tenki.67.7_395. (in Japanese)
- Viale, M., Bianchi, E., Cara, L., Ruiz, L. E., Villalba, R., Pitte, P., Masiokas, M., Rivera, J. and Zalazar, L. (2019): Contrasting climates at both sides of the Andes in Argentina and Chile. *Frontiers in Environmental Science*, **7**, 69, doi: 10.3389/fenvs.2019.00069.
- Yamada, T., Nishimura, H., Suizu, S. and Wakahama, G. (1978): Distribution and process of accumulation and ablation of snow on the west slope of Mt. Asahidake, Hokkaido. *Low Temperature Science Ser. A*, **37**, 1–12. (in Japanese with English summary)
- Yamaguchi, S., Abe, O., Nakai, S. and Sato, A. (2011): Recent fluctuations of meteorological and snow conditions in Japanese mountains. *Annals of Glaciology*, **52**, 209–215, doi: 10.3189/172756411797252266.
- Yoshida, Y. (1960): Snow survey of the catchment basin of the projected Lake Yonezawa. *Geographical Review of Japan Series A*, **33**, 26–43. (in Japanese with English summary)
- Yoshino, M. and Kai, K. (1975): Pressure pattern calendar, 1941–1970. *Tenki*, **22**, 44–49. (in Japanese)